



## 1 Sensitivity of a leaf gas-exchange model for estimating paleoatmospheric CO<sub>2</sub> 2 concentration

3

4 Dana L. Royer<sup>1</sup>, Kylan M. Moynihan<sup>1</sup>, Melissa L. McKee<sup>1</sup>, Liliana Londoño<sup>2</sup>, and Peter J. Franks<sup>3</sup>

5 <sup>1</sup>Department of Earth and Environmental Sciences, Wesleyan University, Middletown, Connecticut, USA

6 <sup>2</sup>Smithsonian Tropical Research Institute, Balboa, Ancón, Republic of Panamá

7 <sup>3</sup>Faculty of Agriculture and Environment, University of Sydney, Sydney, New South Wales, Australia

8 **Correspondence:** Dana L. Royer ([droyer@wesleyan.edu](mailto:droyer@wesleyan.edu))

9

10

11 **Abstract.** Leaf gas-exchange models show considerable promise as paleo-CO<sub>2</sub> proxies. They are largely  
12 mechanistic in nature, provide well-constrained estimates even when CO<sub>2</sub> is high, and can be applied to  
13 most subaerial, stomata-bearing leaves from C<sub>3</sub> taxa, regardless of age or taxonomy. Here we place  
14 additional observational and theoretical constraints on one of these models, the “Franks” model. In  
15 order to gauge the model’s general accuracy in a way that is appropriate for fossil studies, we estimated  
16 CO<sub>2</sub> from 40 species of extant angiosperms, conifers, and ferns based only on measurements that can be  
17 made directly from fossils (leaf δ<sup>13</sup>C and stomatal density and size) and a limited sample size (1-3 leaves  
18 per species). The mean error rate is 28%, which is similar to or better than the accuracy of other leading  
19 paleo-CO<sub>2</sub> proxies. We find that leaf temperature and photorespiration do not strongly affect estimated  
20 CO<sub>2</sub>, although more work is warranted on the possible influence of O<sub>2</sub> concentration on  
21 photorespiration. Leaves from the lowermost 1-2 m of closed-canopy forests should not be used  
22 because the local air δ<sup>13</sup>C value is lower than the global well-mixed value. Such leaves are not common  
23 in the fossil record, but can be identified by morphological and isotopic means.

24

25

### 26 1 Introduction

27

28 Leaves on terrestrial plants are well poised to record information about the concentration of  
29 atmospheric CO<sub>2</sub>. They are in direct contact with the atmosphere and have large surface-area-to-volume  
30 ratios, so the leaf internal CO<sub>2</sub> concentration is tightly coupled to atmospheric CO<sub>2</sub> concentration. Also,  
31 leaves are specifically built for the purpose of fixing atmospheric carbon into structural tissue, and face  
32 constant selection pressure to optimize their carbon uptake relative to water loss. As a result, many  
33 components of the leaf system are sensitive to atmospheric CO<sub>2</sub>, and these components feedback on  
34 one another to reach a new equilibrium when atmospheric CO<sub>2</sub> changes. In terms of carbon assimilation,  
35 Farquhar and Sharkey (1982) modeled this system in its simplest form as:

36

$$37 A_n = g_{c(tot)} \times (c_a - c_i), \quad (1)$$

38

39 where  $A_n$  is the leaf CO<sub>2</sub> assimilation rate ( $\mu\text{mol m}^{-2} \text{s}^{-1}$ ),  $g_{c(tot)}$  is the total operational conductance to CO<sub>2</sub>  
40 diffusion from the atmosphere to site of photosynthesis ( $\text{mol m}^{-2} \text{s}^{-1}$ ),  $c_a$  is atmospheric CO<sub>2</sub>  
41 concentration ( $\mu\text{mol mol}^{-1}$  or ppm), and  $c_i$  is leaf intercellular CO<sub>2</sub> concentration ( $\mu\text{mol mol}^{-1}$  or ppm)  
42 (see also Von Caemmerer, 2000).

43

Rearranging Eq. (1) for atmospheric CO<sub>2</sub> yields:

44

$$45 c_a = \frac{A_n}{g_{c(tot)} \times (1 - \frac{c_i}{c_a})}. \quad (2)$$

46



47 Equation (2) forms the basis of two leaf gas-exchange approaches for estimating paleo-CO<sub>2</sub> from fossils  
 48 (Konrad et al., 2008; Franks et al., 2014; Konrad et al., 2017). In the Franks model, conductance is  
 49 estimated in part from measurements of stomatal size and density,  $c_i/c_a$  from measurements of leaf  $\delta^{13}\text{C}$   
 50 along with reconstructions of coeval air  $\delta^{13}\text{C}$  (see also Eq. 9), and  $A_n$  from knowledge of living relatives  
 51 and its dependency on  $c_a$  (Franks et al., 2014). Following Farquhar et al. (1980), the latter is modeled as  
 52 (Franks et al., 2014; Kowalczyk et al., 2018):

$$54 \quad A_n = A_0 \frac{[\frac{c_i}{c_a}]c_a - \Gamma^*][\frac{c_{i0}}{c_{a0}}]c_{a0} + 2\Gamma^*}{[\frac{c_i}{c_a}]c_a + 2\Gamma^*][\frac{c_{i0}}{c_{a0}}]c_{a0} - \Gamma^*}, \quad (3)$$

55  
 56 where  $\Gamma^*$  is the CO<sub>2</sub> compensation point in the absence of dark respiration (ppm) and the subscript “0”  
 57 refers to conditions at a known CO<sub>2</sub> concentration (typically present-day). Equations (2) and (3) are then  
 58 solved iteratively until the solution for  $c_a$  converges.

59 These gas-exchange approaches grew out of a group of paleo-CO<sub>2</sub> proxies based on the CO<sub>2</sub>  
 60 sensitivity of stomatal density ( $D$ ) or the similar metric stomatal index (Woodward, 1987; Royer, 2001).  
 61 Here, the  $D$ - $c_a$  sensitivity is calibrated in an extant species, allowing paleo-CO<sub>2</sub> inference from the same  
 62 (or very similar) fossil species. These empirical relationships typically follow a power-law function  
 63 (Wynn, 2003; Franks et al., 2014; Konrad et al., 2017):

$$64 \quad c_a = \frac{1}{kD^\alpha}, \quad (4)$$

65  
 66 where  $k$  and  $\alpha$  are species-specific constants.

67 The related stomatal ratio proxy is simplified:  $D$  is measured in an extant species ( $D_0$ , at present-  
 68 day  $c_{a0}$ ) and then the ratio of  $D_0$  to  $D$  in a related fossil species is assumed to be linearly related to the  
 69 ratio of paleo- $c_a$  to present-day  $c_{a0}$  (Chaloner and McElwain, 1997; McElwain, 1998):

$$70 \quad \frac{c_a}{c_{a0}} = k \frac{D_0}{D}. \quad (5)$$

71  
 72 Equation (5) can be rearranged to match Eq. (4) but with  $\alpha$  fixed at 1. Thus, paleo-CO<sub>2</sub> estimates using  
 73 the stomatal ratio proxy are based on a one-point calibration and an assumption that  $\alpha = 1$ ;  
 74 observations do not always support this assumption (e.g.,  $\alpha = 0.43$  for *Ginkgo biloba*; Barclay and Wing,  
 75 2016). The scalar  $k$  was originally set at 2 for Paleozoic and Mesozoic reconstructions so that paleo-CO<sub>2</sub>  
 76 estimates during the Carboniferous matched that from long-term carbon cycle models (Chaloner and  
 77 McElwain, 1997). For younger reconstructions,  $k$  is probably closer to 1 (by definition,  $k = 1$  for present-  
 78 day plants). We note that the stomatal ratio proxy was originally conceived as providing qualitative  
 79 information, only, about paleo-CO<sub>2</sub> (McElwain and Chaloner, 1995, 1996; Chaloner and McElwain, 1997;  
 80 McElwain, 1998) and has not been tested with dated herbaria materials or with CO<sub>2</sub> manipulation  
 81 experiments.

82  
 83 At high CO<sub>2</sub>, the  $D$ - $c_a$  sensitivity saturates, leading to uncertain paleo-CO<sub>2</sub> estimates, often with  
 84 unbounded upper limits (e.g., Smith et al., 2010; Doria et al., 2011). Stomatal density does not respond  
 85 to CO<sub>2</sub> in all species (Woodward and Kelly, 1995; Royer, 2001), and because  $D$ - $c_a$  relationships can be  
 86 species-specific (that is, different species in the same genus with different responses; Beerling, 2005;  
 87 Haworth et al., 2010), only fossil taxa that are still alive today should be used. The gas-exchange proxies  
 88 partly address these limitations: 1) CO<sub>2</sub> estimates remain well-bounded—even at high CO<sub>2</sub>—and their  
 89 precision is similar to or better than other leading paleo-CO<sub>2</sub> proxies (~+35/-25% at 95% confidence;  
 90 Franks et al., 2014); 2) the models are mostly mechanistic; that is, they are explicitly driven by plant



92 physiological principles, not just empirical relationships measured on living plants; 3) because the  
93 models retain sensitivity at high CO<sub>2</sub> and do not require that a fossil species still be alive today, much of  
94 the paleobotanical record is open for CO<sub>2</sub> inference, regardless of age or taxonomy; and 4) because the  
95 models are based on multiple inputs linked by feedbacks, they can still perform adequately even if one  
96 or more of the inputs in a particular taxon is not sensitive to CO<sub>2</sub>, for example stomatal density (Milligan  
97 et al., in review).

98 We note that the published uncertainties (= precision) associated with the stomatal density  
99 proxies are probably too small because they usually only reflect uncertainty in the calibration regression  
100 or in the measured values of fossil stomatal density, but not both; when this is done, errors often  
101 exceed ±30% at 95% confidence (Beerling et al., 2009). Also, error rates in estimates from extant taxa  
102 where CO<sub>2</sub> is known (= accuracy) are usually smaller with the stomatal density proxies (e.g., Barclay and  
103 Wing, 2016), but this is expected because the same taxa have been calibrated in present-day (or near  
104 present-day) conditions. Because the gas-exchange proxies are largely built from physiological  
105 principles, they have less “recency” bias; that is, the gas-exchange proxies estimate present-day and  
106 paleo-CO<sub>2</sub> with similar certainty when the same methods are used to determine the inputs.

107

108

## 109 **2 Study Aims and Methods**

110

111 Leaf gas-exchange proxies for paleo-CO<sub>2</sub> are becoming popular (Konrad et al., 2008; Grein et al.,  
112 2011b; Grein et al., 2011a; Erdei et al., 2012; Roth-Nebelsick et al., 2012; Grein et al., 2013; Franks et al.,  
113 2014; Maxbauer et al., 2014; Roth-Nebelsick et al., 2014; Montañez et al., 2016; Reichgelt et al., 2016;  
114 Konrad et al., 2017; Tesfamichael et al., 2017; Kowalczyk et al., 2018; Lei et al., 2018; Londoño et al.,  
115 2018; Richey et al., 2018; Milligan et al., in review). However, many elements of these models remain  
116 understudied. Here we investigate four such elements for the Franks et al. (2014) model: how does the  
117 model perform across a large number of phylogenetically diverse taxa; and how is the model affected by  
118 temperature, photorespiration, and proximity to the forest floor? We describe next the motivation and  
119 details of the study design.

120

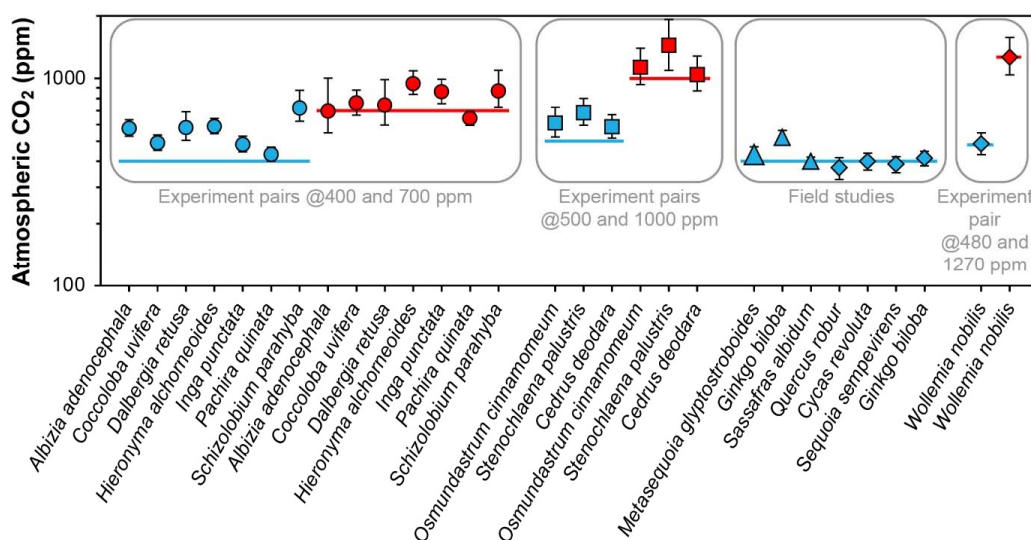
### 121 **2.1 General testing in living plants**

122

123 Franks et al. (2014) tested the model on four species of field-grown trees (three gymnosperms and one  
124 angiosperm) and one conifer grown in chambers at 480 and 1270 ppm CO<sub>2</sub>. The average error rate  
125 (absolute value of estimated CO<sub>2</sub> minus measured CO<sub>2</sub>, divided by measured CO<sub>2</sub>) was 5%. Follow-up  
126 work with three field-grown tree species (Maxbauer et al., 2014; Kowalczyk et al., 2018), CO<sub>2</sub>  
127 experiments on seven tropical trees species (Londoño et al., 2018), and experiments on two fern and  
128 one conifer species (Milligan et al., in review) indicate somewhat higher error rates (Fig. 1). Combined,  
129 the average error rate is 19% (median = 13%).

130

131



132  
 133 **Figure 1.** Published CO<sub>2</sub> estimates using the Franks model for extant plants where the physiological  
 134 inputs  $A_0$  (assimilation rate at a known CO<sub>2</sub> concentration) and/or  $g_{c(op)}/g_{c(max)}$  (ratio of operational to  
 135 maximum leaf conductance to CO<sub>2</sub>) were measured directly. Horizontal lines are the correct CO<sub>2</sub>  
 136 concentrations. Uncertainties in the estimates correspond to the 16<sup>th</sup>-84<sup>th</sup> percentile range. Circles are  
 137 from Londoño et al. (2018), squares from Milligan et al. (in review), large triangle from Maxbauer et al.  
 138 (2014), small triangles from Kowalczyk et al. (2018), and diamonds from Franks et al. (2014).  
 139  
 140

141 In these studies, two of the key physiological inputs were measured directly with an infrared gas  
 142 analyzer: the assimilation rate at a known CO<sub>2</sub> concentration ( $A_0$ ) and/or the ratio of operational to  
 143 maximum stomatal conductance to CO<sub>2</sub> ( $g_{c(op)}/g_{c(max)}$ ), or  $\zeta$ , the latter of which is important for  
 144 calculating the total leaf conductance ( $g_{c(tot)}$ ). These two inputs cannot be directly measured on fossils;  
 145 thus, the error rates associated with Figure 1 may not be representative for fossil studies. Franks et al.  
 146 (2014) argue that within plant functional types growing in their natural environment, mean  $A_0$  is fairly  
 147 conservative, leading to the recommended mean  $A_0$  values in Franks et al. (2014) ( $12 \mu\text{mol m}^{-2} \text{s}^{-1}$  for  
 148 angiosperms, 10 for conifers, and 6 for ferns and ginkgos). Along similar lines, the mean ratio  $g_{c(op)}/g_{c(max)}$   
 149 tends to be conserved across plant functional types; Franks et al. (2014) recommend a value of 0.2,  
 150 which may correspond to the most efficient setpoint for stomata to control conductance (Franks et al.,  
 151 2012). This conservation of physiological function is one of the underlying principles in the Franks  
 152 model.

153 Here we test this assumption by estimating CO<sub>2</sub> from 40 phylogenetically diverse species of  
 154 field-grown trees. In making these estimates, we use the recommended mean values of  $A_0$  and  
 155  $g_{c(op)}/g_{c(max)}$  from Franks et al. (2014) instead of measuring them directly. Thus, this dataset should be a  
 156 more faithful gauge for model accuracy as applied to fossils. Of the 40 species, 21 were previously  
 157 published in Londoño et al. (2018), who collected sun-adapted canopy leaves of angiosperms using a  
 158 crane in Parque Nacional San Lorenzo, Panama. To test the method in temperate forests, we collected  
 159 leaves from eleven angiosperm and seven conifer species from Dinosaur State Park (Rocky Hill,  
 160 Connecticut), Wesleyan University (Middletown, Connecticut), and Connecticut College (New London,



161 Connecticut) during the summer of 2015. Here, all trees grew in open, park-like settings; one to three  
162 sun leaves were sampled from the lower outside crown of each tree. In January of 2015, we also  
163 sampled sun-exposed leaves from the tree fern *Cyathea arborea* in El Yunque National Forest, Puerto  
164 Rico (near the Yokahú Tower).

165 Stomatal size and density were measured either on untreated leaves using epifluorescence  
166 microscopy with a 420-490 nm filter, or on cleared leaves (using 50% household bleach or 5% NaOH)  
167 using transmitted-light microscopy. For most species, whole-leaf  $\delta^{13}\text{C}$  comes from Royer and Hren  
168 (2017); the same leaves were measured for  $\delta^{13}\text{C}$  and stomatal morphology. The UC Davis Stable Isotope  
169 Facility measured some additional leaf samples. Table S1 summarizes for these 40 species all of the  
170 inputs needed to run the Franks model, along with the estimated  $\text{CO}_2$  concentrations. Uncertainties in  
171 the estimates are based on error propagation using Monte Carlo simulations (Franks et al., 2014).

172

173 

## 2.2 Temperature

174

175 The Franks model can be configured for any temperature. Franks et al. (2014) recommend that the  
176 photosynthesis parameters  $A_0$  and  $\Gamma^*$ , and the air physical properties affecting diffusion of  $\text{CO}_2$  into the  
177 leaf (the ratio of  $\text{CO}_2$  diffusivity in air to the molar volume of air, or  $d/v$ ) correspond with the mean  
178 daytime growing-season leaf temperature (more precisely, assimilation-weighted leaf temperature). The  
179 reasoning behind this is that (i) the assimilation-weighted leaf temperature will correspond with the  
180 mean  $c_i/c_a$  derived from fossil leaf  $\delta^{13}\text{C}$ ; and (ii) both theory (Michaletz et al., 2015; Michaletz et al.,  
181 2016) and observations (Helliker and Richter, 2008; Song et al., 2011) indicate that the control of leaf  
182 gas exchange leads to relatively stable assimilation-weighted leaf temperatures ( $\sim 19\text{-}25^\circ\text{C}$  from  
183 temperate to tropical regions) despite large differences in air temperature. This is mostly due to the  
184 effects of transpiration on leaf energy balance. Franks et al. (2014) chose a fixed temperature of  $25^\circ\text{C}$   
185 because much of the Mesozoic and Cenozoic correspond to climates warmer than the present-day.  
186 When applying the Franks model to known cooler paleoenvironments, improved accuracy may be  
187 achieved with leaf-temperature-appropriate values for  $A_0$ ,  $\Gamma^*$ , and  $d/v$ .

188 Bernacchi et al. (2003) proposed the following temperature sensitivity for  $\Gamma^*$  based on  
189 experiments:

190

$$191 \Gamma^* = e^{(19.02 - \frac{37.83}{RT})}, \quad (6)$$

192

193 where  $R$  is the molar gas constant ( $8.31446 \times 10^{-3} \text{ kJ K}^{-1} \text{ mol}^{-1}$ ) and  $T$  is leaf temperature (K). Marrero and  
194 Mason (1972) describe the sensitivity of water vapor diffusivity to temperature as:

195

$$196 d = 1.87 \times 10^{-10} \left( \frac{T^{2.072}}{P} \right), \quad (7)$$

197

198 where  $P$  is atmospheric pressure, which we fix at 1 atmosphere. Lastly, the temperature sensitivity of  
199 the molar volume of air follows ideal gas principles:

200

$$201 v = v_{STP} \left( \frac{T}{T_{STP}} \right) \left( \frac{P}{P_{STP}} \right), \quad (8)$$

202

203 where  $T_{STP}$  is 273.15 K,  $P_{STP}$  is 1 atmosphere, and  $v_{STP}$  is the air volume at  $T_{STP}$  and  $P_{STP}$  ( $0.022414 \text{ m}^3 \text{ mol}^{-1}$ ).

204

205 Using Eqs. (6-8), we can describe how, conceptually, the sensitivities of  $\Gamma^*$  and  $d/v$  to leaf  
206 temperature affect estimates of  $\text{CO}_2$  from the Franks model. We apply these relationships to a suite of



207 409 fossil and extant leaves from 62 species of angiosperms, gymnosperms, and ferns. These data come  
208 from the current study (see Sect. 2.1 and 2.4) and Londoño et al. (2018), Kowalczyk et al. (2018), and  
209 Milligan et al. (in review).

210 To experimentally test more generally how the Franks model is influenced by temperature, we  
211 grew six species of plants inside two growth chambers with contrasting temperatures (Conviron E7/2;  
212 Winnipeg, Canada). Air temperature was 28 °C and 20 °C during the day, and 19 °C and 11 °C during the  
213 night. We note that the difference in leaf temperature was probably smaller than that in air  
214 temperature during the day (8 °C; see earlier discussion). We held fixed the day length (17 hours with a  
215 30 minute simulated dawn and dusk) and CO<sub>2</sub> concentration (500 ppm). Humidity differed moderately  
216 between chambers (76.5 ± 1.8% 1σ and 90.0 ± 3.6%). To minimize any chamber effects, we alternated  
217 plants between chambers every two weeks.

218 Four of the species started as saplings purchased from commercial nurseries: bare-root, one-  
219 foot tall saplings of *Acer negundo* and *Carpinus caroliniana*, one-foot tall saplings of *Ostrya virginiana*  
220 with a soil ball, and bare-root, four-inch tall saplings of *Ilex opaca*. We grew the other two species from  
221 seed: *Betula lenta* from a commercial source, and *Quercus rubra* from a single tree on Wesleyan  
222 University's campus. All seeds were soaked in water for 24 hours and then cold stratified in a  
223 refrigerator for 30 and 60 days, respectively.

224 All seeds and saplings grew in the same potting soil (Promix Bx with Mycorise; Premier  
225 Horticulture; Quakertown, Pennsylvania, USA) and fertilizer (Scotts all-purpose flower and vegetable  
226 fertilizer; Maryville, Ohio, USA). They were watered to field capacity every other day, and we discarded  
227 any excess water passing through the pots. After three months of growth in the chambers, for each  
228 species-chamber pair we harvested the three newest fully expanded leaves whose buds developed  
229 during the experiment. In most cases, we harvested five plants per species-chamber pair; the one  
230 exception was *I. opaca*, where we were limited to three plants in the warm treatment and two in the  
231 cool treatment.

232 We measured stomatal size and density on cleared leaves (using 50% household bleach) with  
233 transmitted-light microscopy. Whole-leaf δ<sup>13</sup>C comes from the UC Davis Stable Isotope Facility and the  
234 Light Stable Isotope Mass Spec Lab at the University of Florida; the same leaves were measured for δ<sup>13</sup>C  
235 and stomatal morphology. Because we used the same CO<sub>2</sub> gas cylinder as Milligan et al. (in review), we  
236 used their two-end-member mixing model to calculate the δ<sup>13</sup>C of the chamber CO<sub>2</sub> at 500 ppm (-10.6  
237 ‰). We used the recommended values from Franks et al. (2014) for the physiological inputs  $A_0$  and  
238  $g_{c(op)}/g_{c(max)}$ . Table S1 summarizes all of the inputs from this experiment needed to run the Franks model,  
239 along with the estimated CO<sub>2</sub> concentrations. The standard errors for the inputs are based on plant  
240 means.

241 To test if leaf δ<sup>13</sup>C and stomatal morphology (stomatal density, stomatal pore length, and single  
242 guard cell width) differed between temperature treatments across species, we implemented a mixed  
243 model in R (R Core Team, 2016) using the lme4 (Bates et al., 2015) and lmerTest (Kuznetsova et al.,  
244 2017) packages, with temperature and species as the two fixed factors. To test if there was a significant  
245 difference between CO<sub>2</sub> estimates from the two temperature treatments, we ran a Kolmogorov–  
246 Smirnov (KS) test in R. For each species, we first estimated CO<sub>2</sub> for each plant in the warm and cool  
247 treatments based on simulated inputs constrained by their means and variances. In the typical case with  
248 five plants per chamber, this produced five CO<sub>2</sub> estimates for the warm chamber and the same for the  
249 cool chamber. A KS test was then used to test for a significant temperature effect. We repeated this  
250 procedure 10,000 times, with 10,000 associated KS tests. The fraction of tests with a p-value < 0.05 was  
251 taken as the overall p value. An advantage of this approach is that it incorporates both within- and  
252 across-plant variation.

253

254





## 255 2.3 Photorespiration

256

 257  $c_i/c_a$  is estimated in the Franks model following Farquhar et al. (1982):

258

259 
$$\Delta_{leaf} = a + (b - a) \times \frac{c_i}{c_a}, \quad (9)$$

260

 261 where  $a$  is the carbon isotope fractionation due to diffusion of  $\text{CO}_2$  in air (4.4‰; Farquhar et al., 1982),  $b$   
 262 is the fractionation associated with RuBP carboxylase (30‰; Roeske and O'Leary, 1984), and  $\Delta_{leaf}$  is the  
 263 net fractionation between air and assimilated carbon ( $[\delta^{13}\text{C}_{air} - \delta^{13}\text{C}_{leaf}]/[1 + \delta^{13}\text{C}_{leaf}/1000]$ ).

 264 Equation (9) can be expanded to include other effects, including photorespiration (Farquhar et  
 265 al., 1982):

266

267 
$$\Delta_{leaf} = a + (b - a) \times \frac{c_i}{c_a} - \frac{f\Gamma^*}{c_a}, \quad (10)$$

268

 269 where  $f$  is the carbon isotope fractionation due to photorespiration. Photorespiration occurs when the  
 270 enzyme rubisco fixes  $\text{O}_2$ , not  $\text{CO}_2$  (i.e., RuBP oxygenase). One product of photorespiration is  $\text{CO}_2$  (Jones,  
 271 1992), whose  $\delta^{13}\text{C}$  is lower than the source substrate glycine. If this respired  $\text{CO}_2$  escapes to the  
 272 atmosphere, the  $\delta^{13}\text{C}$  of the leaf carbon becomes more positive. Thus, if  $c_i/c_a$  is calculated using Eq. (9),  
 273 as is common practice, the calculation may be falsely low, leading to an underprediction of atmospheric  
 274  $\text{CO}_2$ .

 275 Measured values for  $f$  vary from ~9-15‰ (see compilation in Schubert and Jahren, 2018), which  
 276 is in line with theoretical predictions (Tcherkez, 2006). At a 400 ppm atmospheric  $\text{CO}_2$  and  $\Gamma^*$  of 40 ppm,  
 277 Eq. (10) implies that ~1‰ of  $\Delta_{leaf}$  is due to photorespiration, meaning that  $c_i/c_a$  should be ~0.04 higher  
 278 relative to Eq. (9). Here, using the suite of fossil and extant leaves described in Sect. 2.2, we explore how  
 279 the carbon isotopic fractionation associated with photorespiration affects  $\text{CO}_2$  estimates with the Franks  
 280 model. Because  $c_i/c_a$  is present in both of the fundamental equations (Eqs. 2 and 3), we solve them  
 281 iteratively until  $c_i/c_a$  converges.

282

## 283 2.4 Leaves that grow close to the forest floor

284

 285 The composition of air close to the forest floor can differ considerably from the well-mixed atmosphere.  
 286 Of relevance to the Franks model, soil respiration can lead to a locally higher  $\text{CO}_2$  concentration and  
 287 lower  $\delta^{13}\text{C}_{air}$  (Table 1). This effect is strongest at night, when the forest boundary layer is thickest (e.g.,  
 288 Munger and Hadley, 2017), but we focus here on daylight hours because that is when most plants take  
 289 up  $\text{CO}_2$ . In wet tropical forests, which can have very high soil respiration rates,  $\text{CO}_2$  during the day near  
 290 the forest floor can be elevated by tens-of-ppm, and the  $\delta^{13}\text{C}_{air}$  can be 2-3‰ lower; in temperate forests,  
 291 the deviations are smaller (Table 1). Above ~2 m,  $\text{CO}_2$  concentrations and air  $\delta^{13}\text{C}$  during the daytime  
 292 largely match the well-mixed atmosphere.

293

294



295 **Table 1.** Deviations in the  $\delta^{13}\text{C}$  and concentration of  $\text{CO}_2$  close to a forest floor relative to well-mixed air  
 296 above the canopy. All measurements were made close to mid-day.

Study	$\delta^{13}\text{C}_{\text{air}}$ relative to well-mixed air (‰)	$\text{CO}_2$ relative to well-mixed air (ppm)	Height above forest floor (m)	Forest location
<b>Tropical forest</b>				
Broadmeadow et al. (1992)	-2	+20	0.15-1	Trinidad during dry season
Buchmann et al. (1997)	-2	+30	0.70-0.75	French Guiana during wet and dry seasons
Holtum and Winter (2001)	NA	+50	0.10	Panama during wet and dry seasons
Lloyd et al. (1996)	-3	+70	1	Brazil (Amazon Basin)
Quay et al. (1989)	-3	+20	2	Brazil (Amazon Basin)
Sternberg et al. (1989)	-2	+25	1	Panama during wet and dry seasons
<b>Temperate forest</b>				
Francey et al. (1985)	-1	+20	1	Tasmania
Munger and Hadley (2017)	NA	+15	1	Massachusetts (Harvard Forest)

297  
298

299 As a result, leaves that grow close to the forest floor may cause the Franks model to produce  
 300  $\text{CO}_2$  estimates higher than that of the mixed atmosphere for at least two reasons. First, the  
 301 concentration of  $\text{CO}_2$  near the forest floor is elevated; that is, the model may correctly estimate a  $\text{CO}_2$   
 302 concentration that the user is not interested in. Second, because the  $\delta^{13}\text{C}_{\text{air}}$  that a forest-floor plant  
 303 experiences is lower than the global well-mixed value, if the user chooses the well-mixed value for  
 304 model input (inferred, for example, from the  $\delta^{13}\text{C}$  of marine carbonate; Tipple et al., 2010),  $c_i/c_a$  and thus  
 305 atmospheric  $\text{CO}_2$  will be overestimated (see Eq. 2).

306 We sought to test how the Franks model is affected by the forest-floor microenvironment for  
 307 five tropical angiosperm species and fifteen temperate angiosperm and fern species. The tropical leaves  
 308 were sampled at  $\sim 1$ -2 m height from Parque Nacional San Lorenzo, Panama. In contrast to the canopy  
 309 data set from San Lorenzo (Sect. 2.1), these  $\text{CO}_2$  estimates have not been previously reported. In the  
 310 summer of 2015, seven fern species were sampled at  $\sim 0.5$  m height from Connecticut College and  
 311 Wesleyan University. Also, we used leaf vouchers from Royer et al. (2010), who sampled eight  
 312 herbaceous angiosperm species at  $\sim 0.1$ -0.2 m height from Reed Gap, Connecticut. For all 20 species,  
 313 stomatal and carbon isotopic measurements follow the methods described in Sect. 2.1. Table S1  
 314 contains all of the inputs needed to run the Franks model, along with the estimated  $\text{CO}_2$  concentrations.

315 We also investigated if we could include the forest-floor  $\delta^{13}\text{C}_{\text{air}}$  effect in our estimates of  
 316 atmospheric  $\text{CO}_2$ . If the only  $\text{CO}_2$  inputs close to the forest floor are from the soil and well-mixed  
 317 atmosphere, the system can be modeled as a two-endmember mixing model where  $\delta^{13}\text{C}_{\text{air}}$  has a  
 318 positive, linear relationship with  $1/\text{CO}_2$  (Keeling, 1958). If the  $\text{CO}_2$  concentration and  $\delta^{13}\text{C}$  of both  
 319 endmembers are known, the forest-floor microenvironment should fall somewhere on the modelled  
 320 line. Importantly, the Franks model provides a second constraint on the system. Here,  $\delta^{13}\text{C}_{\text{air}}$  has a  
 321 negative, nonlinear relationship with  $1/\text{CO}_2$  because  $\delta^{13}\text{C}_{\text{air}}$  is positively related to  $c_i/c_a$  and  $\text{CO}_2$ . The  
 322 Franks model thus provides a second calculation for the relationship between  $\delta^{13}\text{C}_{\text{air}}$  and estimated  $\text{CO}_2$





323 concentration. The intersection between the two curves should be the correct  $\delta^{13}\text{C}_{\text{air}}$  and  $\text{CO}_2$   
324 concentration for the forest-floor microenvironment.

325 To estimate the soil  $\text{CO}_2$  endmember, we measured the  $\delta^{13}\text{C}$  of soil organic matter collected  
326 from the A horizons of 13 soil sites at San Lorenzo, and of five each at Reed Gap and Connecticut  
327 College. For all soils, we assume a 5000 ppm  $\text{CO}_2$  concentration for a depth that is below the zone of  $\text{CO}_2$   
328 diffusion from the atmosphere ( $\sim 0.3$  m; Cerling, 1999; Breecker et al., 2009). The true value for wet  
329 temperate and tropical forest soils may be somewhat less or substantially more than 5000 ppm (Medina  
330 et al., 1986; Cerling, 1999; Hirano et al., 2003; Hashimoto et al., 2004; Sotta et al., 2004). Because the  
331 mixing model uses  $1/\text{CO}_2$ , a much higher  $\text{CO}_2$  concentration (e.g., 10000 ppm) has little impact on our  
332 results.

333

334

### 335 **3 Results and Discussion**

336

#### 337 **3.1 General testing in living plants**

338

339 Estimates of  $\text{CO}_2$  across the 40 tree species sampled in the field range from 275 to 850 ppm, with a  
340 mean of 478 ppm and median of 472 ppm (Fig. 2). There are no strong differences across taxonomic  
341 orders, nor between leaves from tropical and temperate forests. The mean error rate across the  
342 estimates is 28% (median = 24%), which is higher than estimates that include direct measurements of  
343 the physiological inputs  $A_0$  and  $g_{c(\text{op})}/g_{c(\text{max})}$  (mean = 19%; median = 13%; Fig. 1). Along similar lines, if the  
344 estimates presented in Fig. 1 are re-estimated using the values for  $A_0$  and  $g_{c(\text{op})}/g_{c(\text{max})}$  recommended by  
345 Franks et al. (2014), the mean error rate increases to 31% (median = 21%).

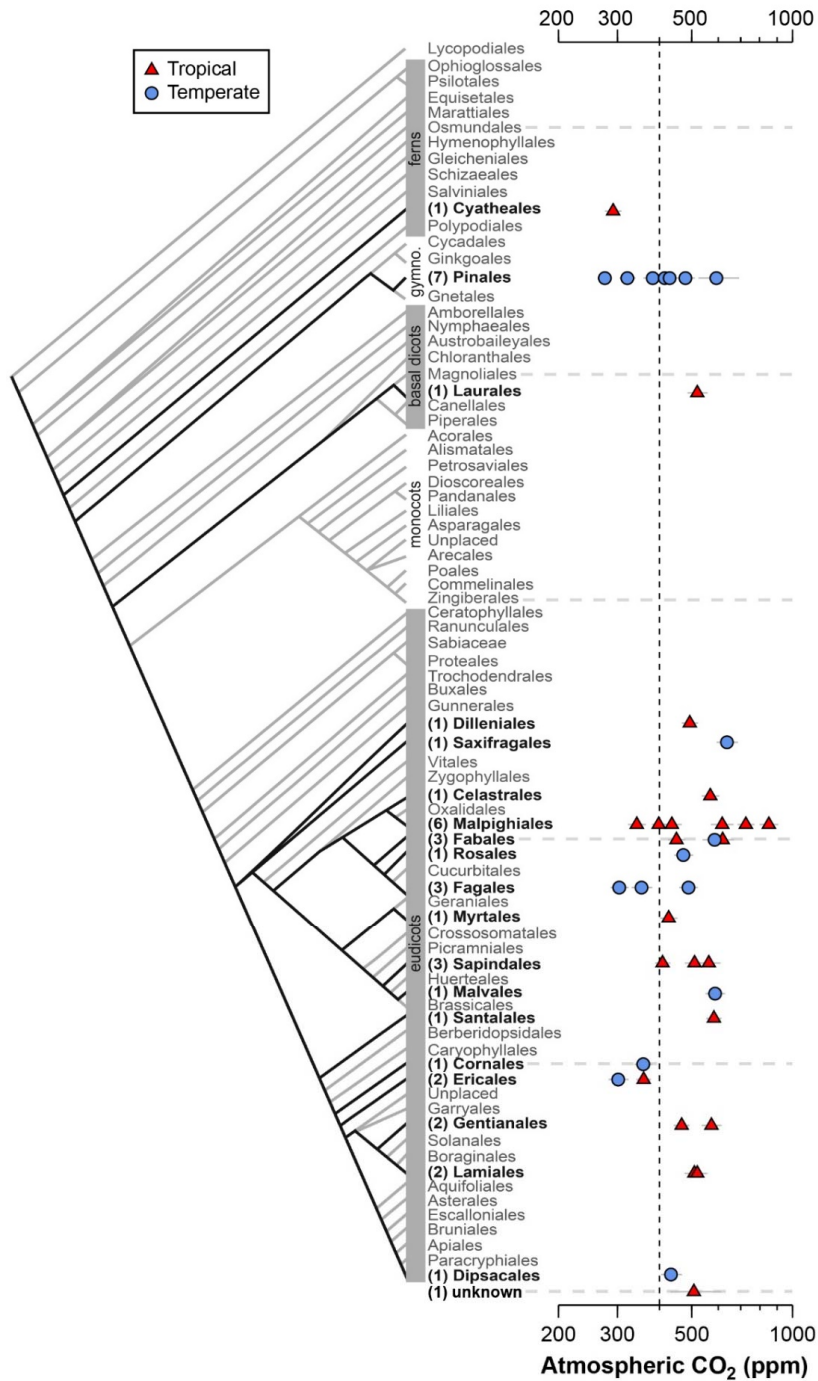
346 These results indicate that  $\text{CO}_2$  accuracy is generally improved when  $A_0$  and/or  $g_{c(\text{op})}/g_{c(\text{max})}$  is  
347 measured. These measurements require expensive gas-exchange equipment and are not always easy or  
348 practical to make. Moreover,  $A_0$  and  $g_{c(\text{op})}/g_{c(\text{max})}$  cannot be measured on fossils. Some gains in accuracy  
349 are possible by measuring  $A_0$  and  $g_{c(\text{op})}/g_{c(\text{max})}$  on extant relatives of the fossil species (e.g., the same  
350 genus). Absent of this, our analysis using the recommended mean values of Franks et al. (2014) indicates  
351 an error rate, on average, of approximately 28%. This is comparable to or better than other leading  
352 paleo- $\text{CO}_2$  proxies (Franks et al., 2014).

353

354 One reliable way to improve accuracy is to estimate  $\text{CO}_2$  with multiple species because the  
355 falsely-high and falsely-low estimates partially cancel each other out. The grand mean of estimates  
356 presented in Fig. 2 (478 ppm) is 20% from the 400 ppm target, which is less than the 28% mean error  
357 rate of individual estimates.

357

358

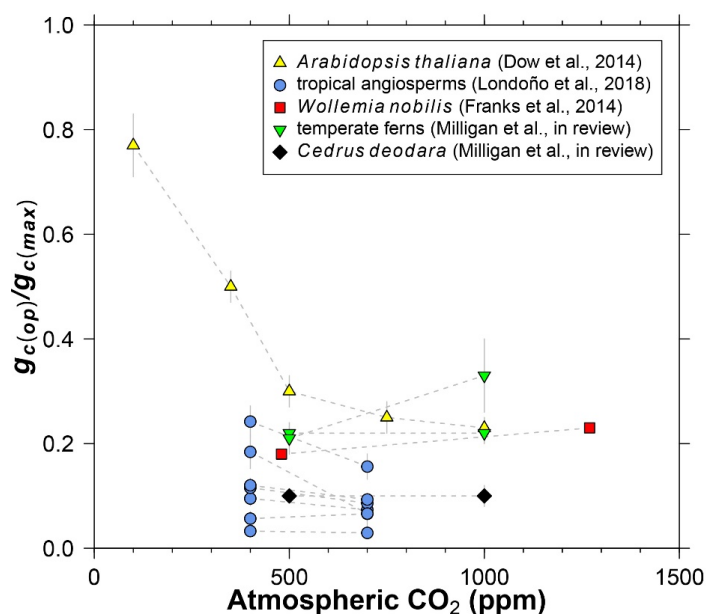


359  
 360 **Figure 2.** Estimates of CO<sub>2</sub> based on canopy leaves from 40 tree species. Uncertainties in the estimates  
 361 correspond to the 16<sup>th</sup>-84<sup>th</sup> percentile range. Vertical line is the correct concentration (400 ppm). On the  
 362 left is an order-level vascular plant phylogeny (APW v.13; Stevens, 2001 onwards).



363  
 364  
 365  
 366  
 367  
 368  
 369  
 370  
 371  
 372  
 373  
 374  
 375  
 376

Dow et al. (2014) observed that  $g_{c(op)}/g_{c(max)}$  inversely varies with  $CO_2$  in *Arabidopsis thaliana*, but primarily at subambient concentrations (yellow triangles in Fig. 3). At elevated  $CO_2$ ,  $g_{c(op)}/g_{c(max)}$  is close to 0.2, which is the value recommended by Franks et al. (2014). Data from eleven species of angiosperms, conifers, and ferns at present-day (or near present-day) and elevated  $CO_2$  concentrations support the view of a limited effect at high  $CO_2$  (Fig. 3; Franks et al., 2014; Londoño et al., 2018; Milligan et al., in review). More data at subambient  $CO_2$  are needed, but for  $CO_2$  concentrations similar to or higher than the present-day, we see no strong reason to include a  $CO_2$  sensitivity in  $g_{c(op)}/g_{c(max)}$ . The rather low values for *Cedrus deodara* and many of the tropical angiosperms (<0.1) are likely due to stress imposed by their growth chamber environment; these  $g_{c(op)}/g_{c(max)}$  values are probably not representative of field-grown trees, which tend to be closer to 0.2 (Franks et al., 2014).

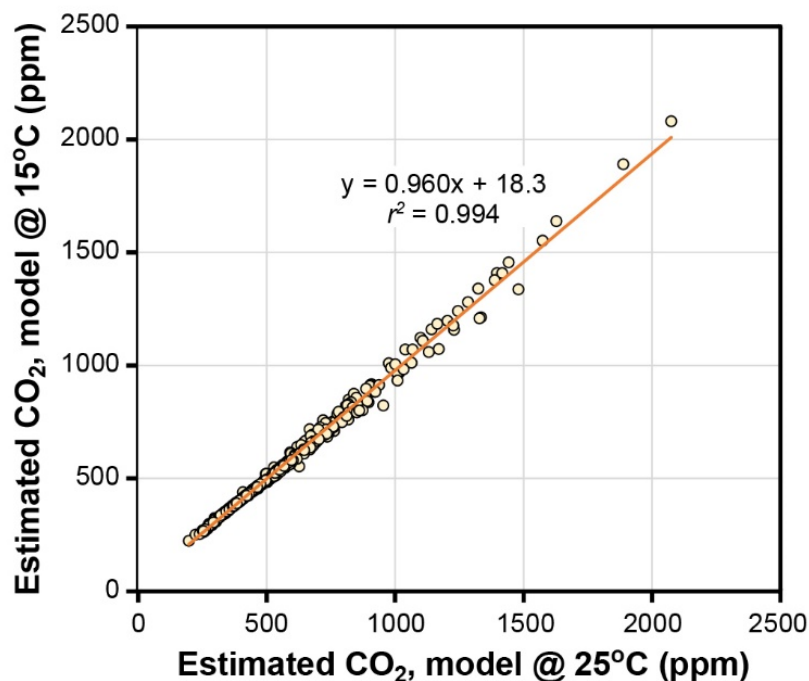


377  
 378  
 379  
 380  
 381  
 382  
 383  
 384  
 385  
 386  
 387  
 388  
 389  
 390  
 391

**Figure 3.** Literature compilation of the sensitivity of  $g_{c(op)}/g_{c(max)}$  (ratio of operational to maximum leaf conductance to  $CO_2$ ) to atmospheric  $CO_2$  concentration.

### 3.2 Temperature

The temperature sensitivities of the ratio of diffusivity of  $CO_2$  in air to the molar volume of air ( $d/v$ ) and the  $CO_2$  compensation point in the absence of dark respiration ( $\Gamma^*$ ) have little effect on estimated  $CO_2$  in the Franks model (Fig. 4). Given that assimilation-weighted leaf temperature only varies about 7 °C across plants today, the differences shown in Fig. 4—which are based on leaf temperatures of 25 °C and 15 °C—are likely a maximum effect. As such, we consider the use of a fixed leaf temperature (e.g., 25 °C) in the model to be a defensible simplification.



392  
393  
394  
395  
396  
397  
398  
399  
400  
401  
402  
403  
404  
405  
406  
407  
408  
409  
410  
411  
412  
413  
414  
415  
416  
417

**Figure 4.** Estimates of CO<sub>2</sub> at leaf temperatures of 25 °C and 15 °C. Each symbol is an extant or fossil leaf. The difference in estimated CO<sub>2</sub> for any leaf is due to the theoretical effects of temperature on gas diffusion ( $d/v$ ) and the CO<sub>2</sub> compensation point in the absence of dark respiration ( $\Gamma^*$ ) (Eqs. 6-8).

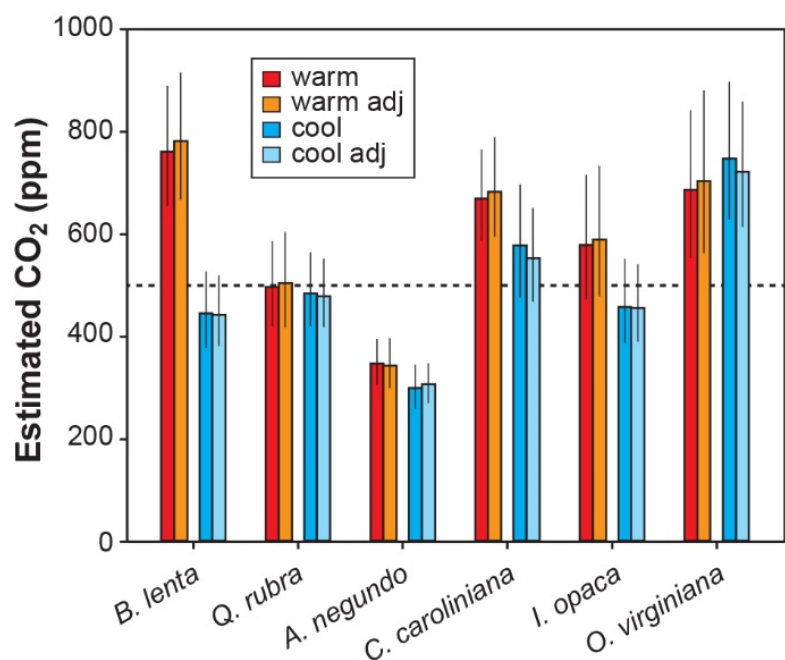
Other inputs in the model may respond to temperature, though. In our growth chamber experiments where daytime air temperatures were 28 °C and 20 °C, the effect on estimated CO<sub>2</sub> was mixed (Fig. 5). In five out of six species, estimated CO<sub>2</sub> was higher in the warm treatment, but for all species these differences were not statistically significant ( $P > 0.05$  based on a KS test; see Methods). Incorporating the temperature sensitivities in  $d/v$  and  $\Gamma^*$  had little effect (“adj” estimates in Fig. 5), as expected from Fig. 4.

None of the measured inputs—stomatal density, stomatal pore length, single guard cell width, and leaf  $\delta^{13}\text{C}$ —were significantly affected by temperature across all species ( $P > 0.05$  for each of the four inputs based on a mixed model; see Methods). These small differences probably cannot account for the differences in estimated CO<sub>2</sub> between temperatures. It is more likely that some of the inputs that we did not directly measure, such as assimilation rate ( $A_0$ ), the  $g_{c(op)}/g_{c(max)}$  ratio, or mesophyll conductance ( $g_m$ ), differ from the true mean value. In the cases for the five species where estimated CO<sub>2</sub> is higher in the warm treatment, our mean  $A_0$  for the warm plants must be falsely high, or  $g_{c(op)}/g_{c(max)}$  or  $g_m$  falsely low.

In summary, we see no strong reason to expand the parameterization of temperature in the model, though more growth-chamber experiments may be warranted. We note that the across-species means of estimated CO<sub>2</sub> for the warm and cool treatments are reasonably close to the 500 ppm target (590 and 502 ppm, respectively) and overall have a mean error rate of 25%. This level of uncertainty is similar to our field estimates where we did not measure  $A_0$  or  $g_{c(op)}/g_{c(max)}$  (28%; see Fig. 2). This too provides support for our recommendation that it is not critical to include a broader treatment of temperature in the model.



418  
419



420  
421 **Figure 5.** Estimates of CO<sub>2</sub> for plants grown inside growth chambers at daytime air temperatures of 28 °C  
422 and 20 °C. Also shown are estimates after taking into account the temperature sensitivity of gas  
423 diffusion ( $d/v$ ) and the CO<sub>2</sub> compensation point in the absence of dark respiration ( $\Gamma^*$ ) (“adj”; see also  
424 Fig. 4). Dashed line is the correct CO<sub>2</sub> concentration (500 ppm). Uncertainties in the estimates  
425 correspond to the 16<sup>th</sup>-84<sup>th</sup> percentile range.

426

427

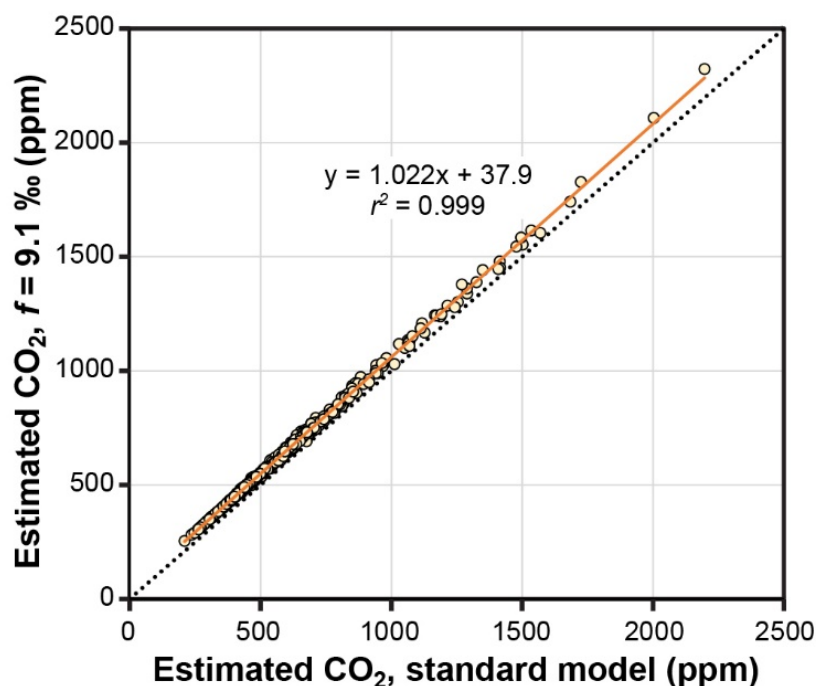
### 428 3.3 Photorespiration

429

430 The theoretical effects of photorespiration do not strongly impact estimates of CO<sub>2</sub> in the Franks model.  
431 The average effect for our 409 extant and fossil leaves is to increase estimated CO<sub>2</sub> by 2.2% plus 38 ppm  
432 (Fig. 6). At 1000 ppm, for example, estimates would increase by 60 ppm. This calculation assumes a  
433 photorespiration fractionation ( $f$ ) of 9.1‰, which is the value estimated for *Arabidopsis thaliana*  
434 (Schubert and Jahren, 2018). If a fractionation towards the upper bound of published estimates is used  
435 instead (15‰), estimated CO<sub>2</sub> increases on average by 3.8% plus 61 ppm. Across this range in  $f$ , the  
436 associated uncertainty in estimated CO<sub>2</sub> is well within the method’s overall precision (~+35/-25% at 95%  
437 confidence; Franks et al., 2014). As such, CO<sub>2</sub> estimates made without these photorespiration effects  
438 (i.e. using Eq. 9 instead of Eq. 10) should be reliable, although some improvement is possible using Eq.  
439 10 in cases where  $f$  is accurately known.

440

441



442  
 443 **Figure 6.** Estimates of CO<sub>2</sub> with and without a photorespiration effect ( $f = 9.1‰$ ; see Eq. 10). Each  
 444 symbol is an extant or fossil leaf. Dashed line is  $y=x$ .  
 445

446  
 447 We note that both  $f$  and  $\Gamma^*$  are also affected by atmospheric O<sub>2</sub> concentration. Because O<sub>2</sub> is  
 448 directly responsible for photorespiration,  $f$  should scale with O<sub>2</sub> (or, more precisely, the O<sub>2</sub>:CO<sub>2</sub> molar  
 449 ratio). Unfortunately, this effect is poorly constrained (Beerling et al., 2002; Berner et al., 2003; Porter et  
 450 al., 2017). In contrast, the theoretical effect of O<sub>2</sub> on  $\Gamma^*$  is known: it is linear with a slope of 0.5 (Farquhar  
 451 et al., 1982; see their Eq. B13). During the Phanerozoic, O<sub>2</sub> likely ranged from 10-30%, with lows during  
 452 the early Paleozoic and early Triassic, and highs during the Carboniferous to early Permian and  
 453 Cretaceous (Berner, 2009; Glasspool and Scott, 2010; Arvidson et al., 2013; Mills et al., 2016; Lenton et  
 454 al., 2018). Assuming a present-day  $\Gamma^*$  of 40 ppm (at 21% O<sub>2</sub>),  $\Gamma^*$  would be 49 ppm at 30% O<sub>2</sub> and 29 ppm  
 455 at 10% O<sub>2</sub>. Running the Franks model on our library of 409 extant and fossil leaves, we find little effect  
 456 on estimated CO<sub>2</sub>: estimates are 3.3% higher on average at 30% O<sub>2</sub> than at 10% O<sub>2</sub>.  
 457

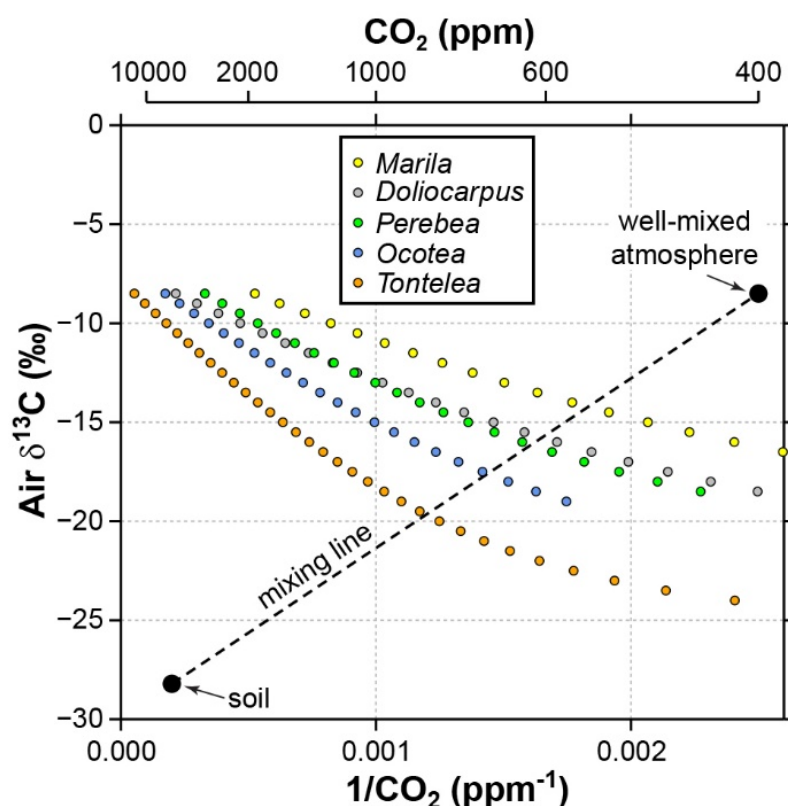
### 458 3.4 Leaves that grow close to the forest floor

459  
 460 CO<sub>2</sub> estimates for tropical understory leaves from five species at San Lorenzo, Panama, are very high,  
 461 ranging from 1903 to 18863 ppm (species mean = 6837 ppm). For two of the species Londoño et al.  
 462 (2018) also analyzed canopy leaves from trees nearby, and these within-species comparisons highlight  
 463 the vast discrepancy (*Ocotea* sp.: 541 vs. 5737 ppm; *Tantelea* sp.: 622 vs. 18863 ppm). The primary  
 464 difference in the inputs between the canopy and understory leaves is the  $\delta^{13}\text{C}_{\text{leaf}}$ : Londoño et al. (2018)  
 465 report a species-mean  $\delta^{13}\text{C}_{\text{leaf}}$  of -30.0‰ for the 21 canopy species versus -35.6‰ for the five understory  
 466 species. This difference leads to very different mean estimates of  $c_i/c_a$ : 0.69 for canopy leaves versus a  
 467 highly unrealistic (Diefendorf et al., 2010) 0.93 for understory leaves.





468 It is likely that the high CO<sub>2</sub> estimates from understory leaves are mostly driven by falsely high  
 469 δ<sup>13</sup>C<sub>air</sub> inputs. Following the mixing model strategy outlined in Sect. 2.4 (and based on a soil organic  
 470 matter δ<sup>13</sup>C of -28.2‰ measured at San Lorenzo), we calculate a species-mean δ<sup>13</sup>C<sub>air</sub> of -16.7‰ (mean  
 471 of intersection points in Fig. 7). When this δ<sup>13</sup>C<sub>air</sub> is used to estimate CO<sub>2</sub> with the Franks model (instead  
 472 of -8.5‰), the species mean drops to 699 ppm. This is somewhat higher than the species mean from  
 473 canopy leaves in the same forest (563 ppm; red triangles in Fig. 2; Londoño et al., 2018).  
 474  
 475



476 **Figure 7.** Sensitivity of estimated CO<sub>2</sub> in the Franks model to the δ<sup>13</sup>C of atmospheric CO<sub>2</sub>. Estimates  
 477 come from leaves of five angiosperm species that grew close to the forest floor in Parque Nacional San  
 478 Lorenzo, Panama. The step in δ<sup>13</sup>C<sub>air</sub> between estimates is 0.5‰. The dashed line is a two-endmember  
 479 mixing model for CO<sub>2</sub> between the soil and well-mixed atmosphere. The intersection between the  
 480 mixing model and the Franks model should correspond to the CO<sub>2</sub> concentration and δ<sup>13</sup>C<sub>air</sub> of the  
 481 forest-floor microenvironment.  
 482

483  
 484

485 Understory leaves from Connecticut temperate forests show similar but less dramatic patterns,  
 486 which we attribute to a more open canopy with stronger atmospheric mixing. CO<sub>2</sub> estimates for the 15  
 487 species range from 447 to 1567 ppm (mean = 794 ppm). Our intersection method identifies a mean  
 488 δ<sup>13</sup>C<sub>air</sub> of -11.2‰ for the Wesleyan and Connecticut College campuses (based on a soil δ<sup>13</sup>C of -27.6‰  
 489 measured at Connecticut College) and -10.3‰ for Reed Gap (soil δ<sup>13</sup>C = -26.4‰). Using these adjusted



490  $\delta^{13}\text{C}_{\text{air}}$ , the species mean of estimated  $\text{CO}_2$  drops to 566 ppm, which is somewhat higher than the species  
491 mean from canopy leaves in the same areas (449 ppm; blue circles in Fig. 2).

492 We acknowledge that this analysis is too simple: other factors probably contribute to the  
493 differences in estimated  $\text{CO}_2$  between canopy and understory leaves. Our predicted  $\delta^{13}\text{C}_{\text{air}}$  values are too  
494 low ( $\sim 8\text{‰}$  and  $2\text{‰}$  lower than the well-mixed atmosphere for the tropical and temperate forests) and  
495 our estimated  $\text{CO}_2$  too high ( $\sim 100$  ppm higher than that from canopy leaves). In the lowermost 1-2  
496 meters of the canopy, previous work suggests up to a  $-3\text{‰}$  and  $+70$  ppm deviation in tropical forests and  
497  $-1\text{‰}$  /  $+20$  ppm in temperate forests (Table 1). One input that could help to resolve this discrepancy is  
498 the assimilation rate ( $A_0$ ). We assumed a fixed  $A_0$  of  $12 \mu\text{mol m}^{-2} \text{s}^{-1}$  for all leaves, regardless of canopy  
499 position. Shade leaves often have lower assimilation rates than sun leaves (Givnish, 1988). Substituting  
500 lower  $A_0$  values for understory leaves would lower estimated  $\text{CO}_2$  roughly in proportion (Eqs. 2-3). Using  
501 lower  $A_0$  values for shade leaves in the model is appropriate, but determining the best value is difficult.  
502 Typical  $A_0$  values for leaves growing at the top of the canopy in full sun are far more consistent because  
503 photosynthesis in these leaves is usually at its maximum capacity (saturated at full sunlight) for the  
504 prevailing atmospheric  $\text{CO}_2$  concentration. Because the degree of shadiness near the forest floor is  
505 highly variable, photosynthesis ( $A_0$ ) in these leaves will be acclimated to some fraction of the full-sun  
506 maximum in a sun exposed leaf, but careful thought must go into determining what this fraction is.

507 We note that our mixing-model strategy cannot be applied to fossils because the global  
508 atmospheric  $\text{CO}_2$  concentration is needed (one endpoint for dashed line in Fig. 7). Instead, our  
509 motivation for the analysis is to demonstrate that: 1) leaves growing in the lowermost 2 m of the canopy  
510 should be considered with caution in the context of the Franks model; and 2) the failure of the model is  
511 due to faulty inputs (mostly  $\delta^{13}\text{C}_{\text{air}}$ ), not the model itself.

512 In most fossil leaf deposits, shade morphotypes are comparatively rare (e.g., Kürschner, 1997;  
513 Wang et al., in press) because—relative to sun leaves—they are not as tough, do not travel as far by  
514 wind, and are produced at a slower rate (Dilcher, 1973; Roth and Dilcher, 1978; Spicer, 1980; Ferguson,  
515 1985; Burnham et al., 1992). Our recommendation is to exclude such leaves. There are several ways to  
516 differentiate sun vs. shade morphotypes: overall shape (Talbert and Holch, 1957; Givnish, 1978;  
517 Kürschner, 1997; Sack et al., 2006), shape of epidermal cells (larger and with a more undulated outline in  
518 shade leaves; Kürschner, 1997; Dunn et al., 2015), vein density (lower in shade leaves; Uhl and  
519 Mosbrugger, 1999; Sack and Scoffoni, 2013; Crifo et al., 2014; Londoño et al., 2018), and range in  $\delta^{13}\text{C}_{\text{leaf}}$   
520 (high when both sun and shade leaves are present, for example in our study; Graham et al., 2014). Not  
521 all shade leaves grow within 2 m of the forest floor, but excluding all such leaves would eliminate the  
522 forest-floor bias.

523

524

#### 525 4 Conclusions

526

527 The Franks model is reasonably accurate ( $\sim 28\%$  error rate) even when the physiological inputs  $A_0$   
528 (assimilation rate at a known  $\text{CO}_2$  concentration) and  $g_{c(\text{op})}/g_{c(\text{max})}$  (ratio of operational to maximum leaf  
529 conductance to  $\text{CO}_2$ ) are inferred, not measured. Accuracy does improve when these inputs are  
530 measured ( $\sim 19\%$  error rate), but such measurements are not possible with fossils and may not always  
531 be feasible with nearest living relatives. A 28% error rate is broadly in line with (or better than) other  
532 leading paleo- $\text{CO}_2$  proxies.

533 Most of the possible confounding factors that we investigated appear minor. The temperature  
534 sensitivities of  $d/v$  (related to gas diffusion) and  $\Gamma^*$  ( $\text{CO}_2$  compensation point in the absence of dark  
535 respiration) have a negligible impact on estimated  $\text{CO}_2$ . Our temperature experiments in growth  
536 chambers point to larger differences in some species, which must be related to incorrect values for  
537 inputs that were not directly measured, such as  $A_0$ ,  $g_{c(\text{op})}/g_{c(\text{max})}$ , and  $g_m$  (mesophyll conductance).



538 Overall, though, we find that the differences in estimated CO<sub>2</sub> imparted by temperature are generally  
539 smaller than the overall 28% error rate.

540 Incorporating the covariance between CO<sub>2</sub> concentration and photorespiration leads to only  
541 small changes in estimated CO<sub>2</sub>. O<sub>2</sub> concentration affects photorespiration and thus may confound CO<sub>2</sub>  
542 estimates from the Franks model, but presently the effect is poorly quantified. The effect of O<sub>2</sub> on  $f^*$  is  
543 better known, and imparts only small changes in estimated CO<sub>2</sub> across a feasible range in Phanerozoic  
544 O<sub>2</sub> of 10-30%.

545 Leaves from the lowermost 1-2 m of the canopy experience slightly elevated CO<sub>2</sub> concentrations  
546 and lower air  $\delta^{13}\text{C}$  during the daytime relative to the well-mixed atmosphere. We find that if we use the  
547 well-mixed air  $\delta^{13}\text{C}$  to estimate CO<sub>2</sub> from leaves that grew near the forest floor, estimates are too high,  
548 especially in dense tropical canopies. When we use a two-endmember mixing model to calculate the  
549 correct local air  $\delta^{13}\text{C}$ , the falsely-high CO<sub>2</sub> estimates largely disappear. For fossil applications, shade  
550 leaves from the bottom of the canopy should be avoided. Shade leaves are typically rare in the fossil  
551 record (relative to sun leaves), and can be identified by their overall shape, the shape of their epidermal  
552 cells, their low leaf  $\delta^{13}\text{C}$ , and their low vein density.

553 Conceptually, the Franks model holds considerable promise for quantifying paleo-CO<sub>2</sub>: it is  
554 mechanistically grounded and can be applied to most fossil leaves. Our tests of the model's accuracy  
555 and sensitivity to temperature and photorespiration largely uphold this promise.

556

557

558 **Author contribution.** DR, KM, MM, and LL designed and conducted the experiments; all authors  
559 interpreted the data; DR prepared the manuscript with contributions from all co-authors.

560

561 **Competing interests.** The authors declare that they have no conflict of interest.

562

563 **Acknowledgements.** We thank G. Dreyer and P. Siver for logistical support at Connecticut College, S.  
564 Wang for lab assistance, and C. Crifò and A. Baresh for collecting the tropical samples. Support for LL  
565 was provided by the Smithsonian Tropical Research Institute; the Mark Tupper Fellowship; National  
566 Science Foundation grants EAR 0824299 and OISE, EAR, DRL 0966884; the Anders Foundation; and the  
567 Gregory D. and Jennifer Walston Johnson and 1923 Fund.

568

569

570

571

## 571 References

572 Arvidson, R. S., Mackenzie, F. T., and Guidry, M. W.: Geologic history of seawater: A MAGic approach to  
573 carbon chemistry and ocean ventilation, *Chemical Geology*, 362, 287-304,

574 <https://doi.org/10.1016/j.chemgeo.2013.10.012>, 2013.

575 Barclay, R. S. and Wing, S. L.: Improving the *Ginkgo* CO<sub>2</sub> barometer: implications for the early Cenozoic  
576 atmosphere, *Earth and Planetary Science Letters*, 439, 158-171,

577 <https://doi.org/10.1016/j.epsl.2016.01.012>, 2016.

578 Bates, D., Mächler, M., Bolker, B., and Walker, S.: Fitting linear mixed-effects models using lme4, *Journal*  
579 *of Statistical Software*, 67, doi:10.18637/jss.v18067.i18601,

580 <https://doi.org/10.18637/jss.v067.i01>, 2015.

581 Beerling, D. J.: Evolutionary responses of land plants to atmospheric CO<sub>2</sub>, in: *A History of Atmospheric*  
582 *CO<sub>2</sub> and Its Effects on Plants, Animals, and Ecosystems*, edited by: Ehleringer, J. R., Cerling, T. E.,  
583 and Dearing, M. D., Springer, New York, 114-132, 2005.



- 584 Beerling, D. J., Lake, J. A., Berner, R. A., Hickey, L. J., Taylor, D. W., and Royer, D. L.: Carbon isotope  
585 evidence implying high O<sub>2</sub>/CO<sub>2</sub> ratios in the Permo-Carboniferous atmosphere, *Geochimica et*  
586 *Cosmochimica Acta*, 66, 3757-3767, [https://doi.org/10.1016/S0016-7037\(02\)00901-8](https://doi.org/10.1016/S0016-7037(02)00901-8), 2002.
- 587 Beerling, D. J., Fox, A., and Anderson, C. W.: Quantitative uncertainty analyses of ancient atmospheric  
588 CO<sub>2</sub> estimates from fossil leaves, *American Journal of Science*, 309, 775-787,  
589 <https://doi.org/10.2475/09.2009.01>, 2009.
- 590 Bernacchi, C. J., Pimentel, C., and Long, S. P.: *In vivo* temperature response functions of parameters  
591 required to model RuBP-limited photosynthesis, *Plant, Cell & Environment*, 26, 1419-1430,  
592 <https://doi.org/10.1046/j.0016-8025.2003.01050.x>, 2003.
- 593 Berner, R. A.: Phanerozoic atmospheric oxygen: new results using the GEOCARBSULF model, *American*  
594 *Journal of Science*, 309, 603-606, <https://doi.org/10.2475/07.2009.03>, 2009.
- 595 Berner, R. A., Beerling, D. J., Dudley, R., Robinson, J. M., and Wildman, R. A.: Phanerozoic atmospheric  
596 oxygen, *Annual Review of Earth and Planetary Sciences*, 31, 105-134,  
597 <https://doi.org/10.1146/annurev.earth.31.100901.141329>, 2003.
- 598 Breecker, D. O., Sharp, Z. D., and McFadden, L. D.: Seasonal bias in the formation and stable isotopic  
599 composition of pedogenic carbonate in modern soils from central New Mexico, USA, *Geological*  
600 *Society of America Bulletin*, 121, 630-640, <https://doi.org/10.1130/B26413.1>, 2009.
- 601 Broadmeadow, M., Griffiths, H., Maxwell, C., and Borland, A.: The carbon isotope ratio of plant organic  
602 material reflects temporal and spatial variations in CO<sub>2</sub> within tropical forest formations in  
603 Trinidad, *Oecologia*, 89, 435-441, <https://doi.org/10.1007/BF00317423>, 1992.
- 604 Buchmann, N., Guehl, J.-M., Barigah, T., and Ehleringer, J. R.: Interseasonal comparison of CO<sub>2</sub>  
605 concentrations, isotopic composition, and carbon dynamics in an Amazonian rainforest (French  
606 Guiana), *Oecologia*, 110, 120-131, <https://doi.org/10.1007/s004420050140>, 1997.
- 607 Burnham, R. J., Wing, S. L., and Parker, G. G.: The reflection of deciduous forest communities in leaf  
608 litter: implications for autochthonous litter assemblages from the fossil record, *Paleobiology*, 18,  
609 30-49, <https://doi.org/10.1017/S0094837300012203>, 1992.
- 610 Cerling, T. E.: Stable carbon isotopes in palaeosol carbonates, *Special Publications of the International*  
611 *Association of Sedimentologists*, 27, 43-60, 1999.
- 612 Chaloner, W. G. and McElwain, J.: The fossil plant record and global climatic change, *Review of*  
613 *Palaeobotany and Palynology*, 95, 73-82, [https://doi.org/10.1016/S0034-6667\(96\)00028-0](https://doi.org/10.1016/S0034-6667(96)00028-0),  
614 1997.
- 615 Crifò, C., Currano, E. D., Baresch, A., and Jaramillo, C.: Variations in angiosperm leaf vein density have  
616 implications for interpreting life form in the fossil record, *Geology*, 42, 919-922,  
617 <https://doi.org/10.1130/g35828.1>, 2014.
- 618 Diefendorf, A. F., Mueller, K. E., Wing, S. L., Koch, P. L., and Freeman, K. H.: Global patterns in leaf <sup>13</sup>C  
619 discrimination and implications for studies of past and future climate, *Proceedings of the*  
620 *National Academy of Sciences, USA*, 107, 5738-5743, <https://doi.org/10.1073/pnas.0910513107>,  
621 2010.
- 622 Dilcher, D. L.: A paleoclimatic interpretation of the Eocene floras of southeastern North America, in:  
623 *Vegetation and Vegetational History of Northern Latin America*, edited by: Graham, A., Elsevier,  
624 Amsterdam, 39-53, 1973.
- 625 Doria, G., Royer, D. L., Wolfe, A. P., Fox, A., Westgate, J. A., and Beerling, D. J.: Declining atmospheric  
626 CO<sub>2</sub> during the late Middle Eocene climate transition, *American Journal of Science*, 311, 63-75,  
627 <https://doi.org/10.2475/01.2011.03>, 2011.
- 628 Dow, G. J., Bergmann, D. C., and Berry, J. A.: An integrated model of stomatal development and leaf  
629 physiology, *New Phytologist*, 201, 1218-1226, <https://doi.org/10.1111/nph.12608>, 2014.



- 630 Dunn, R. E., Strömberg, C. A. E., Madden, R. H., Kohn, M. J., and Carlini, A. A.: Linked canopy, climate,  
631 and faunal change in the Cenozoic of Patagonia, *Science*, 347, 258-261,  
632 <https://doi.org/10.1126/science.1260947>, 2015.
- 633 Erdei, B., Utescher, T., Hably, L., Tamás, J., Roth-Nebelsick, A., and Grein, M.: Early Oligocene continental  
634 climate of the Palaeogene Basin (Hungary and Slovenia) and the surrounding area, *Turkish*  
635 *Journal of Earth Sciences*, 21, 153-186, <https://doi.org/10.3906/yer-1005-29>, 2012.
- 636 Farquhar, G. D. and Sharkey, T. D.: Stomatal conductance and photosynthesis, *Annual Review of Plant*  
637 *Physiology*, 33, 317-345, <https://doi.org/10.1146/annurev.pp.33.060182.001533>, 1982.
- 638 Farquhar, G., von Caemmerer, S., and Berry, J.: A biochemical model of photosynthetic CO<sub>2</sub> assimilation  
639 in leaves of C<sub>3</sub> species, *Planta*, 149, 78-90, <https://doi.org/10.1007/BF00386231>, 1980.
- 640 Farquhar, G. D., O'Leary, M. H., and Berry, J. A.: On the relationship between carbon isotope  
641 discrimination and the intercellular carbon dioxide concentration in leaves, *Australian Journal of*  
642 *Plant Physiology*, 9, 121-137, <https://doi.org/10.1071/PP9820121>, 1982.
- 643 Ferguson, D. K.: The origin of leaf-assemblages—new light on an old problem, *Review of Palaeobotany*  
644 *and Palynology*, 46, 117-188, [https://doi.org/10.1016/0034-6667\(85\)90041-7](https://doi.org/10.1016/0034-6667(85)90041-7), 1985.
- 645 Francey, R., Gifford, R., Sharkey, T., and Weir, B.: Physiological influences on carbon isotope  
646 discrimination in huon pine (*Lagarostrobos franklinii*), *Oecologia*, 66, 211-218,  
647 <https://doi.org/10.1007/BF00379857>, 1985.
- 648 Franks, P. J., Leitch, I. J., Ruzsala, E. M., Hetherington, A. M., and Beerling, D. J.: Physiological framework  
649 for adaptation of stomata to CO<sub>2</sub> from glacial to future concentrations, *Philosophical*  
650 *Transactions of the Royal Society B*, 367, 537-546, <https://doi.org/10.1098/rstb.2011.0270>,  
651 2012.
- 652 Franks, P. J., Royer, D. L., Beerling, D. J., Van de Water, P. K., Cantrill, D. J., Barbour, M. M., and Berry, J.  
653 A.: New constraints on atmospheric CO<sub>2</sub> concentration for the Phanerozoic, *Geophysical*  
654 *Research Letters*, 41, 4685-4694, <https://doi.org/10.1002/2014gl060457>, 2014.
- 655 Givnish, T. J.: Ecological aspects of plant morphology: leaf form in relation to environment, *Acta*  
656 *Biotheoretica*, 27, 83-142, 1978.
- 657 Givnish, T. J.: Adaptation to sun and shade: a whole-plant perspective, *Australian Journal of Plant*  
658 *Physiology*, 15, 63-92, <https://doi.org/10.1071/PP9880063>, 1988.
- 659 Glasspool, I. J. and Scott, A. C.: Phanerozoic concentrations of atmospheric oxygen reconstructed from  
660 sedimentary charcoal, *Nature Geoscience*, 3, 627-630, <https://doi.org/10.1038/ngeo923>, 2010.
- 661 Graham, H. V., Patzkowsky, M. E., Wing, S. L., Parker, G. G., Fogel, M. L., and Freeman, K. H.: Isotopic  
662 characteristics of canopies in simulated leaf assemblages, *Geochimica et Cosmochimica Acta*,  
663 144, 82-95, <https://doi.org/10.1016/j.gca.2014.08.032>, 2014.
- 664 Grein, M., Utescher, T., Wilde, V., and Roth-Nebelsick, A.: Reconstruction of the middle Eocene climate  
665 of Messel using palaeobotanical data, *Neues Jahrbuch Für Geologie und Paläontologie*  
666 *Abhandlungen*, 260, 305-318, <https://doi.org/10.1127/0077-7749/2011/0139>, 2011a.
- 667 Grein, M., Konrad, W., Wilde, V., Utescher, T., and Roth-Nebelsick, A.: Reconstruction of atmospheric  
668 CO<sub>2</sub> during the early Middle Eocene by application of a gas exchange model to fossil plants from  
669 the Messel Formation, Germany, *Palaeogeography Palaeoclimatology Palaeoecology*, 309, 383-  
670 391, <https://doi.org/10.1016/j.palaeo.2011.07.008>, 2011b.
- 671 Grein, M., Oehm, C., Konrad, W., Utescher, T., Kunzmann, L., and Roth-Nebelsick, A.: Atmospheric CO<sub>2</sub>  
672 from the late Oligocene to early Miocene based on photosynthesis data and fossil leaf  
673 characteristics, *Palaeogeography Palaeoclimatology Palaeoecology*, 374, 41-51,  
674 <https://doi.org/10.1016/j.palaeo.2012.12.025>, 2013.
- 675 Hashimoto, S., Tanaka, N., Suzuki, M., Inoue, A., Takizawa, H., Kosaka, I., Tanaka, K., Tantasirin, C., and  
676 Tangtham, N.: Soil respiration and soil CO<sub>2</sub> concentration in a tropical forest, Thailand, *Journal of*  
677 *Forest Research*, 9, 75-79, <https://doi.org/10.1007/s10310-003-0046-y>, 2004.





- 678 Haworth, M., Heath, J., and McElwain, J. C.: Differences in the response sensitivity of stomatal index to  
679 atmospheric CO<sub>2</sub> among four genera of Cupressaceae conifers, *Annals of Botany*, 105, 411-418,  
680 <https://doi.org/10.1093/aob/mcp309>, 2010.
- 681 Helliker, B. R. and Richter, S. L.: Subtropical to boreal convergence of tree-leaf temperatures, *Nature*,  
682 454, 511-514, <https://doi.org/10.1038/nature07031>, 2008.
- 683 Hirano, T., Kim, H., and Tanaka, Y.: Long-term half-hourly measurement of soil CO<sub>2</sub> concentration and  
684 soil respiration in a temperate deciduous forest, *Journal of Geophysical Research*, 108, 4631,  
685 <https://doi.org/10.1029/2003JD003766>, 2003.
- 686 Holtum, J. and Winter, K.: Are plants growing close to the floors of tropical forests exposed to markedly  
687 elevated concentrations of carbon dioxide?, *Australian Journal of Botany*, 49, 629-636,  
688 <https://doi.org/10.1071/BT00054>, 2001.
- 689 Jones, H. G.: *Plants and Microclimate*, Cambridge University Press, Cambridge, 1992.
- 690 Keeling, C. D.: The concentration and isotopic abundances of atmospheric carbon dioxide in rural areas,  
691 *Geochimica et Cosmochimica Acta*, 13, 322-334, [https://doi.org/10.1016/0016-7037\(58\)90033-](https://doi.org/10.1016/0016-7037(58)90033-4)  
692 [4](https://doi.org/10.1016/0016-7037(58)90033-4), 1958.
- 693 Konrad, W., Roth-Nebelsick, A., and Grein, M.: Modelling of stomatal density response to atmospheric  
694 CO<sub>2</sub>, *Journal of Theoretical Biology*, 253, 638-658, <https://doi.org/10.1016/j.jtbi.2008.03.032>,  
695 2008.
- 696 Konrad, W., Katul, G., Roth-Nebelsick, A., and Grein, M.: A reduced order model to analytically infer  
697 atmospheric CO<sub>2</sub> concentration from stomatal and climate data, *Advances in Water Resources*,  
698 104, 145-157, <https://doi.org/10.1016/j.advwatres.2017.03.018>, 2017.
- 699 Kowalczyk, J. B., Royer, D. L., Miller, I. M., Anderson, C. W., Beerling, D. J., Franks, P. J., Grein, M.,  
700 Konrad, W., Roth-Nebelsick, A., Bowering, S. A., Johnson, K. R., and Ramezani, J.: Multiple proxy  
701 estimates of atmospheric CO<sub>2</sub> from an early Paleocene rainforest, *Paleoceanography and*  
702 *Paleoclimatology*, <https://doi.org/10.1029/2018PA003356>, 2018.
- 703 Kürschner, W. M.: The anatomical diversity of recent and fossil leaves of the durmast oak (*Quercus*  
704 *petraea* Lieblein/*Q. pseudocastanea* Goeppert)-implications for their use as biosensors of  
705 palaeoatmospheric CO<sub>2</sub> levels, *Review of Palaeobotany and Palynology*, 96, 1-30,  
706 [https://doi.org/10.1016/S0034-6667\(96\)00051-6](https://doi.org/10.1016/S0034-6667(96)00051-6), 1997.
- 707 Kuznetsova, A., Brockhoff, P. B., and Christensen, R. H. B.: lmerTest package: tests in linear mixed effects  
708 models, *Journal of Statistical Software*, 82, <https://doi.org/10.18637/jss.v082.i13>, 2017.
- 709 Lei, X., Du, Z., Du, B., Zhang, M., and Sun, B.: Middle Cretaceous pCO<sub>2</sub> variation in Yumen, Gansu  
710 Province and its response to the climate events, *Acta Geologica Sinica*, 92, 801-813,  
711 <https://doi.org/doi:10.1111/1755-6724.13555>, 2018.
- 712 Lenton, T. M., Daines, S. J., and Mills, B. J. W.: COPSE reloaded: an improved model of biogeochemical  
713 cycling over Phanerozoic time, *Earth-Science Reviews*, 178, 1-28,  
714 <https://doi.org/10.1016/j.earscirev.2017.12.004>, 2018.
- 715 Lloyd, J., Kruijt, B., Hollinger, D. Y., Grace, J., Francey, R. J., Wong, S.-C., Kelliher, F. M., Miranda, A. C.,  
716 Farquhar, G. D., and Gash, J.: Vegetation effects on the isotopic composition of atmospheric CO<sub>2</sub>  
717 at local and regional scales: theoretical aspects and a comparison between rain forest in  
718 Amazonia and a boreal forest in Siberia, *Australian Journal of Plant Physiology*, 23, 371-399,  
719 <https://doi.org/10.1071/PP9960371>, 1996.
- 720 Londoño, L., Royer, D. L., Jaramillo, C., Escobar, J., Foster, D. A., Cárdenas-Rozo, A. L., and Wood, A.:  
721 Early Miocene CO<sub>2</sub> estimates from a Neotropical fossil assemblage exceed 400 ppm, *American*  
722 *Journal of Botany*, <https://doi.org/10.1002/ajb2.1187>, 2018.
- 723 Marrero, T. R. and Mason, E. A.: Gaseous diffusion coefficients, *Journal of Physical and Chemical*  
724 *Reference Data*, 1, 3-118, <https://doi.org/10.1063/1.3253094>, 1972.





- 725 Maxbauer, D. P., Royer, D. L., and LePage, B. A.: High Arctic forests during the middle Eocene supported  
726 by moderate levels of atmospheric CO<sub>2</sub>, *Geology*, 42, 1027-1030,  
727 <https://doi.org/10.1130/g36014.1>, 2014.
- 728 McElwain, J. C.: Do fossil plants signal palaeoatmospheric CO<sub>2</sub> concentration in the geological past?,  
729 *Philosophical Transactions of the Royal Society London B*, 353, 83-96,  
730 <https://doi.org/10.1098/rstb.1998.0193>, 1998.
- 731 McElwain, J. C. and Chaloner, W. G.: Stomatal density and index of fossil plants track atmospheric  
732 carbon dioxide in the Palaeozoic, *Annals of Botany*, 76, 389-395,  
733 <https://doi.org/10.1006/anbo.1995.1112>, 1995.
- 734 McElwain, J. C. and Chaloner, W. G.: The fossil cuticle as a skeletal record of environmental change,  
735 *Palaios*, 11, 376-388, <https://doi.org/10.2307/3515247>, 1996.
- 736 Medina, E., Montes, G., Cuevas, E., and Rokzandic, Z.: Profiles of CO<sub>2</sub> concentration and δ<sup>13</sup>C values in  
737 tropical rain forests of the upper Rio Negro Basin, Venezuela, *Journal of Tropical Ecology*, 2, 207-  
738 217, <https://doi.org/10.1017/S0266467400000821>, 1986.
- 739 Michaletz, S. T., Weiser, M. D., Zhou, J., Kaspary, M., Helliker, B. R., and Enquist, B. J.: Plant  
740 thermoregulation: energetics, trait-environment interactions, and carbon economics, *Trends in*  
741 *Ecology & Evolution*, 30, 714-724, <https://doi.org/10.1016/j.tree.2015.09.006>, 2015.
- 742 Michaletz, S. T., Weiser, M. D., McDowell, N. G., Zhou, J., Kaspary, M., Helliker, B. R., and Enquist, B. J.:  
743 The energetic and carbon economic origins of leaf thermoregulation, *Nature Plants*, 2, 16129,  
744 <https://doi.org/10.1038/nplants.2016.129>, 2016.
- 745 Milligan, J. N., Royer, D. L., Franks, P. J., Upchurch, G. R., and McKee, M. L.: No evidence for a large  
746 atmospheric CO<sub>2</sub> spike across the Cretaceous-Paleogene boundary, *Geophysical Research*  
747 *Letters*, in review.
- 748 Mills, B. J. W., Belcher, C. M., Lenton, T. M., and Newton, R. J.: A modeling case for high atmospheric  
749 oxygen concentrations during the Mesozoic and Cenozoic, *Geology*, 44, 1023-1026,  
750 <https://doi.org/10.1130/g38231.1>, 2016.
- 751 Montañez, I. P., McElwain, J. C., Poulsen, C. J., White, J. D., DiMichele, W. A., Wilson, J. P., Griggs, G., and  
752 Hren, M. T.: Climate, *p*<sub>CO<sub>2</sub></sub> and terrestrial carbon cycle linkages during late Palaeozoic glacial-  
753 interglacial cycles, *Nature Geoscience*, 9, 824-828, <https://doi.org/10.1038/ngeo2822>, 2016.
- 754 Munger, W. and Hadley, J.: CO<sub>2</sub> profile at Harvard Forest HEM and LPH towers since 2009, Harvard  
755 Forest Data Archive: HF197,  
756 <http://harvardforest.fas.harvard.edu:8080/exist/apps/datasets/showData.html?id=hf197>, 2017.
- 757 Porter, A. S., Yiotis, C., Montañez, I. P., and McElwain, J. C.: Evolutionary differences in Δ<sup>13</sup>C detected  
758 between spore and seed bearing plants following exposure to a range of atmospheric O<sub>2</sub>:CO<sub>2</sub>  
759 ratios: implications for paleoatmosphere reconstruction, *Geochimica et Cosmochimica Acta*,  
760 213, 517-533, <https://doi.org/10.1016/j.gca.2017.07.007>, 2017.
- 761 Quay, P., King, S., Wilbur, D., Wofsy, S., and Rickey, J.: <sup>13</sup>C/<sup>12</sup>C of atmospheric CO<sub>2</sub> in the Amazon Basin:  
762 forest and river sources, *Journal of Geophysical Research*, 94, 18327-18336,  
763 <https://doi.org/10.1029/JD094iD15p18327>, 1989.
- 764 R Core Team: R: A Language and Environment for Statistical Computing, R Foundation for Statistical  
765 Computing, Vienna, Austria, <https://www.R-project.org/>, 2016.
- 766 Reichgelt, T., D'Andrea, W. J., and Fox, B. R. S.: Abrupt plant physiological changes in southern New  
767 Zealand at the termination of the Mi-1 event reflect shifts in hydroclimate and *p*CO<sub>2</sub>, *Earth and*  
768 *Planetary Science Letters*, 455, 115-124, <https://doi.org/10.1016/j.epsl.2016.09.026>, 2016.
- 769 Richey, J. D., Upchurch, G. R., Montañez, I. P., Lomax, B. H., Suarez, M. B., Crout, N. M. J., Joeckel, R. M.,  
770 Ludvigson, G. A., and Smith, J. J.: Changes in CO<sub>2</sub> during Ocean Anoxic Event 1d indicate  
771 similarities to other carbon cycle perturbations, *Earth and Planetary Science Letters*, 491, 172-  
772 182, <https://doi.org/10.1016/j.epsl.2018.03.035>, 2018.



- 773 Roeske, C. and O'Leary, M. H.: Carbon isotope effects on enzyme-catalyzed carboxylation of ribulose  
774 bisphosphate, *Biochemistry*, 23, 6275-6284, <https://doi.org/10.1021/bi00320a058>, 1984.
- 775 Roth-Nebelsick, A., Grein, M., Utescher, T., and Konrad, W.: Stomatal pore length change in leaves of  
776 *Eotrigonobalanus furcinervis* (Fagaceae) from the Late Eocene to the Latest Oligocene and its  
777 impact on gas exchange and CO<sub>2</sub> reconstruction, *Review of Palaeobotany and Palynology*, 174,  
778 106-112, <https://doi.org/10.1016/j.revpalbo.2012.01.001>, 2012.
- 779 Roth-Nebelsick, A., Oehm, C., Grein, M., Utescher, T., Kunzmann, L., Friedrich, J.-P., and Konrad, W.:  
780 Stomatal density and index data of *Platanus neptuni* leaf fossils and their evaluation as a CO<sub>2</sub>  
781 proxy for the Oligocene, *Review of Palaeobotany and Palynology*, 206, 1-9,  
782 <https://doi.org/10.1016/j.revpalbo.2014.03.001>, 2014.
- 783 Roth, J. and Dilcher, D.: Some considerations in leaf size and leaf margin analysis of fossil leaves, *Courier*  
784 *Forschungsinstitut Senckenberg*, 30, 165-171, 1978.
- 785 Royer, D. L.: Stomatal density and stomatal index as indicators of paleoatmospheric CO<sub>2</sub> concentration,  
786 *Review of Palaeobotany and Palynology*, 114, 1-28, [https://doi.org/10.1016/S0034-](https://doi.org/10.1016/S0034-6667(00)00074-9)  
787 [6667\(00\)00074-9](https://doi.org/10.1016/S0034-6667(00)00074-9), 2001.
- 788 Royer, D. L. and Hren, M. T.: Carbon isotopic fractionation between whole leaves and cuticle, *Palaios*, 32,  
789 199-205, <https://doi.org/10.2110/palo.2016.073>, 2017.
- 790 Royer, D. L., Miller, I. M., Peppe, D. J., and Hickey, L. J.: Leaf economic traits from fossils support a weedy  
791 habit for early angiosperms, *American Journal of Botany*, 97, 438-445,  
792 <https://doi.org/10.3732/ajb.0900290>, 2010.
- 793 Sack, L. and Scoffoni, C.: Leaf venation: structure, function, development, evolution, ecology and  
794 applications in the past, present and future, *New Phytologist*, 198, 983-1000,  
795 <https://doi.org/10.1111/nph.12253>, 2013.
- 796 Sack, L., Melcher, P. J., Liu, W. H., Middleton, E., and Pardee, T.: How strong is intracanalopy leaf plasticity  
797 in temperate deciduous trees?, *American Journal of Botany*, 93, 829-839,  
798 <https://doi.org/10.3732/ajb.93.6.829>, 2006.
- 799 Schubert, B. A. and Jahren, A. H.: Incorporating the effects of photorespiration into terrestrial  
800 paleoclimate reconstruction, *Earth-Science Reviews*, 177, 637-642,  
801 <https://doi.org/10.1016/j.earscirev.2017.12.008>, 2018.
- 802 Smith, R. Y., Greenwood, D. R., and Basinger, J. F.: Estimating paleoatmospheric pCO<sub>2</sub> during the Early  
803 Eocene Climatic Optimum from stomatal frequency of *Ginkgo*, Okanagan Highlands, British  
804 Columbia, Canada, *Palaeogeography Palaeoclimatology Palaeoecology*, 293, 120-131,  
805 <https://doi.org/10.1016/j.palaeo.2010.05.006>, 2010.
- 806 Song, X., Barbour, M. M., Saurer, M., and Helliker, B. R.: Examining the large-scale convergence of  
807 photosynthesis-weighted tree leaf temperatures through stable oxygen isotope analysis of  
808 multiple data sets, *New Phytologist*, 192, 912-924, [https://doi.org/10.1111/j.1469-](https://doi.org/10.1111/j.1469-8137.2011.03851.x)  
809 [8137.2011.03851.x](https://doi.org/10.1111/j.1469-8137.2011.03851.x), 2011.
- 810 Sotta, E. D., Meir, P., Malhi, Y., Donato nobre, A., Hodnett, M., and Grace, J.: Soil CO<sub>2</sub> efflux in a tropical  
811 forest in the central Amazon, *Global Change Biology*, 10, 601-617,  
812 <https://doi.org/10.1111/j.1529-8817.2003.00761.x>, 2004.
- 813 Spicer, R. A.: The importance of depositional sorting to the biostratigraphy of plant megafossils, in:  
814 *Biostratigraphy of Fossil Plants: Successional and Paleoecological Analyses*, edited by: Dilcher, D.  
815 and Taylor, T., Dowden, Hutchinson, and Ross, Stroudsburg, PA, 171-183, 1980.
- 816 Sternberg, L., Mulkey, S. S., and Wright, S. J.: Ecological interpretation of leaf carbon isotope ratios:  
817 influence of respired carbon dioxide, *Ecology*, 70, 1317-1324, <https://doi.org/10.2307/1938191>,  
818 1989.
- 819 Stevens, P. F.: Angiosperm Phylogeny Website. Version 13., [www.mobot.org/MOBOT/research/APweb/](http://www.mobot.org/MOBOT/research/APweb/),  
820 2001 onwards.



- 821 Talbert, C. M. and Holch, A. E.: A study of the lobing of sun and shade leaves, *Ecology*, 38, 655-658,  
822 <https://doi.org/10.2307/1943135>, 1957.
- 823 Tcherkez, G.: How large is the carbon isotope fractionation of the photorespiratory enzyme glycine  
824 decarboxylase?, *Functional Plant Biology*, 33, 911-920, <https://doi.org/10.1071/FP06098>, 2006.
- 825 Tesfamichael, T., Jacobs, B., Tabor, N., Michel, L., Currano, E., Feseha, M., Barclay, R., Kappelman, J., and  
826 Schmitz, M.: Settling the issue of “decoupling” between atmospheric carbon dioxide and global  
827 temperature: [CO<sub>2</sub>]<sub>atm</sub> reconstructions across the warming Paleogene-Neogene divide, *Geology*,  
828 45, 999-1002, <https://doi.org/10.1130/G39048.1>, 2017.
- 829 Tipple, B. J., Meyers, S. R., and Pagani, M.: Carbon isotope ratio of Cenozoic CO<sub>2</sub>: a comparative  
830 evaluation of available geochemical proxies, *Paleoceanography*, 25, PA3202,  
831 <https://doi.org/10.1029/2009PA001851>, 2010.
- 832 Uhl, D. and Mosbrugger, V.: Leaf venation density as a climate and environmental proxy: a critical review  
833 and new data, *Palaeogeography Palaeoclimatology Palaeoecology*, 149, 15-26,  
834 [https://doi.org/10.1016/S0031-0182\(98\)00189-8](https://doi.org/10.1016/S0031-0182(98)00189-8), 1999.
- 835 Von Caemmerer, S.: *Biochemical Models of Leaf Photosynthesis*, CSIRO Publishing, Collingwood,  
836 Australia, 2000.
- 837 Wang, Y., Ito, A., Huang, Y., Fukushima, T., Wakamatsu, N., and Momohara, A.: Reconstruction of  
838 altitudinal transportation range of leaves based on stomatal evidence: an example of the Early  
839 Pleistocene *Fagus* leaf fossils from central Japan, *Palaeogeography, Palaeoclimatology,*  
840 *Palaeoecology*, <https://doi.org/10.1016/j.palaeo.2018.06.011>, in press.
- 841 Woodward, F. I.: Stomatal numbers are sensitive to increases in CO<sub>2</sub> from pre-industrial levels, *Nature*,  
842 327, 617-618, <https://doi.org/10.1038/327617a0>, 1987.
- 843 Woodward, F. I. and Kelly, C. K.: The influence of CO<sub>2</sub> concentration on stomatal density, *New*  
844 *Phytologist*, 131, 311-327, <https://doi.org/10.1111/j.1469-8137.1995.tb03067.x>, 1995.
- 845 Wynn, J. G.: Towards a physically based model of CO<sub>2</sub>-induced stomatal frequency response, *New*  
846 *Phytologist*, 157, 391-398, <https://doi.org/10.1046/j.1469-8137.2003.00702.x>, 2003.